

000 001 002 003 004 005 006 007 008 009 010 011 LIPSCHITZ-GUIDED MONTE CARLO TREE SEARCH 012 WITH KNOWLEDGE TRANSFER ACROSS SEQUENTIAL 013 TASKS

014 **Anonymous authors**
015 Paper under double-blind review
016
017
018
019
020
021
022
023
024
025
026
027

028 ABSTRACT

029
030 Monte Carlo Tree Search (MCTS) has proven highly effective in solving complex
031 planning tasks by balancing exploration and exploitation using Upper Confidence
032 Bound for Trees (UCT). However, existing works have not considered MCTS-
033 based lifelong planning facing a sequence of MDPs – e.g., each MDP with varying
034 transition probabilities and rewards from previous ones – throughout the operational
035 lifetime. This paper presents LiZero for Lipschitz lifelong planning using MCTS.
036 We propose a novel concept of adaptive UCT (aUCT) to transfer knowledge from
037 previous tasks to the exploration/exploitation of a new task, depending on both the
038 Lipschitz continuity between tasks and the confidence of knowledge in Monte Carlo
039 action sampling. We analyze LiZero’s acceleration factor in terms of improved
040 sampling efficiency and also develop efficient algorithms to compute aUCT in an
041 online fashion by both data-driven and model-based approaches, whose sampling
042 complexity and error bounds are also characterized. Numerical results show that
043 LiZero significantly outperforms existing MCTS and lifelong learning baselines in
044 terms of much faster convergence (3~4x). Our results highlight the potential of
045 LiZero to advance decision-making and planning in dynamic environments.

046 1 INTRODUCTION

047 Monte Carlo Tree Search (MCTS) has demonstrated state-of-the-art performance in solving many
048 challenging planning tasks, from playing the game of Go Silver et al. (2016) and chess to logistic
049 planning Silver et al. (2017). It performs look-ahead searches based on Monte Carlo sampling of
050 the actions to balance efficient exploration and optimized exploitation in the large search space.
051 Recent efforts have focused on developing MCTS algorithms for real-world domains that require the
052 elimination of certain standard assumptions. Examples include MuZero Schrittwieser et al. (2020b)
053 that leverages the decoding of hidden states to avoid requiring the knowledge of the game dynamics;
054 and MAzero Liu et al. (2024) that performs multi-agent search through decentralized execution.
055 Existing work have not considered MCTS with lifelong task-to-task variations, by retaining and
056 transferring prior knowledge to bootstrap lifelong learning across a continuous stream of tasks.

057 We consider MCTS-based lifelong planning under task-to-task variation. An agent faces a series of
058 changing planning tasks – e.g., with varying transition probabilities and rewards – which are drawn
059 sequentially throughout the operational lifetime. Transferring knowledge from prior experience to
060 continually adapt Monte Carlo sampling of the actions and thus speed up searches in new tasks
061 is a key question in this setting. We note that although continual and lifelong planning has been
062 studied in reinforcement learning (RL) context, e.g., learning models of the a task sequence of distinct
063 stationary environments Xie et al. (2020), identifying reusable skills Lu et al. (2020), or estimating
064 Bayesian sampling posteriors Fu et al. (2022), such prior works do not apply to MCTS. Monte Carlo
065 action sampling in MCTS relies on Upper Confidence Tree (UCT) or Predictor Upper Confidence
066 Tree (pUCT) Auger et al. (2013); Matsuzaki (2018) to balance exploration and exploitation in large
067 search spaces. To the best of our knowledge, there has not been existing work analyzing the transfer
068 of knowledge from past MCTS searches to new tasks, thus enabling adaptive UCT/pUCT rules in
069 lifelong MCTS.

This paper proposes LiZero for Lipschitz lifelong planning using MCTS. We quantify a novel concept that the amount of knowledge transferable from a source task to the UCT/pUCT rule of a new task depends on both the similarity between the tasks as well as the confidence of the knowledge. More precisely, by defining a distance metric between two MDPs, we refine the concentration argument and drive a new adaptive UCT bound (denoted as aUCT in this paper) for lifelong MCTS. The aUCT is shown to consist of two components – relating to (i) the Lipschitz continuity between the two tasks and (ii) the confidence of knowledge due to the number of samples in Monte Carlo action sampling. Our results enable the development of a novel LiZero algorithm that makes use of prior experience to run an adaptive MCTS by simulating/traversing from the root node and selecting actions according to the aUCT rule, until reaching a leaf node. We also analyze aUCT’s acceleration factor in terms of improved sampling efficiency due to cross-task transfer. It is shown that smaller task distance and higher confidence can both lead to higher acceleration in aUCT.

To support the practical deployment of LiZero in lifelong planning, we need efficient solutions to compute aUCT in an online fashion. To this end, we develop practical algorithms to estimate various terms in aUCT, and especially the distance metric between two MDPs, from either available state-action samples using a data-driven approach or a parameterized distance using a model-based (deep learning) approach. We provide rigorous analysis on the sampling complexity of the data-driven approach, to ensure arbitrarily small errors with high probability, by modeling a sequence of policy update process by a filtration – i.e., an increasing sequence of σ -algebras. For the model-based approach, we obtain an upper bound using a parameterized distance of the neural network models. These results enable effective LiZero applications to open world tasks. We evaluate LiZero on a series of learning tasks with varying transition probabilities and rewards. LiZero is shown to significantly outperform MCTS and lifelong RL baselines (e.g., Winands (2024); Kocsis & Szepesvári (2006); Cheng et al.; Schrittwieser et al. (2020a); Brafman & Tennenholtz (2002); Lecarpentier et al. (2021a)) in terms of performance, faster convergence to higher optimal rewards. Using the knowledge of only a few source tasks, LiZero achieves 3~4x speedup with about 31% higher early reward in the first half of the learning process.

Our key contributions are as follows. First, we study theoretically the transfer of past experience in MCTS and develop a novel aUCT rule, depending on both Lipschitz continuity between tasks and the confidence of knowledge in Monte Carlo action sampling. It is proven to provide positive acceleration in MCTS due to cross-task transfer. Second, we develop LiZero for lifelong MCTS planning, with efficient methods for online estimation of aUCT and analytical error bounds. Finally, LiZero achieves significant speed-up over MCTS and lifelong RL baselines in lifelong planning.

2 BACKGROUND

Monte Carlo Tree Search (MCTS) Kocsis & Szepesvári (2006); Silver et al. (2016); Schrittwieser et al. (2020b) is a heuristic algorithm for solving problems modeled as Markov Decision Processes (MDPs). It dynamically balances exploration and exploitation by expanding a search tree, simulating action outcomes, and updating value estimates accordingly. An MDP is typically defined as $\langle \mathcal{S}, \mathcal{A}, R, P \rangle$, where \mathcal{S} and \mathcal{A} are the state and action spaces, R_s^a is the reward, and P denotes the transition dynamics.

In the MCTS framework, Upper Confidence Bound for Trees (UCT) Coulom (2006) and its variant, Predictor UCT (pUCT) Matsuzaki (2018); Auger et al. (2013), are widely used to balance exploration and exploitation during node selection. While effective under static assumptions, they perform suboptimally in dynamic, a task sequence of distinct stationary environments where state transitions and rewards change over time Pourshamsaei & Nobakhti (2024); Hernandez-Leal et al. (2017); Goldberg & Matarić (2003). In this paper, we consider MCTS- based lifelong planning, where an agent faces a sequence of distinct MDPs – e.g., with varying transition probabilities and reward – and requires the development of new adaptive UCT bounds.

Lifelong reinforcement learning (RL) Lecarpentier et al. (2021b); Xie et al. (2020); Fu et al. (2022); Lu et al. (2020); Auger et al. (2013) addresses learning a sequence of tasks from unknown MDPs in an online manner. Each sampled MDP is treated as a standalone RL problem where the agent learns and adapts its policy π to maximize expected return Da Silva et al. (2018); Hawasly & Ramamoorthy (2013); Abel et al. (2018). We can reasonably believe that the knowledge gained in similar MDPs can be reused. While prior work explores task modeling Xie et al. (2020), skill reuse Lu et al. (2020), and

108 Bayesian transfer Fu et al. (2022), these methods do not extend naturally to lifelong MCTS, which
 109 requires adaptive UCT-style bounds to enable knowledge transfer and efficient planning across a
 110 sequence of distinct tasks (MDPs).

111

112 3 OUR PROPOSED SOLUTION

114 3.1 DERIVING ADAPTIVE UPPER CONFIDENCE BOUND (AUCT)

116 To derive the proposed aUCT rule, we consider a set of m past known MDPs $\mathcal{M}_1, \dots, \mathcal{M}_m$ and
 117 their learned search policies π_1, \dots, π_m . Let S and A be their state and action spaces, respectively¹,
 118 $N_i(s, a)$ be the visit count of MDP \mathcal{M}_i to state-action pair $(s \in S, a \in A)$, $W_i(s, a)$ to denote its
 119 sampled return, and $Q_{\mathcal{M}_i}^{N_i}(s, a) = W_i(s, a)/N_i(s, a)$ be the learned estimate for the Q-value of MDP
 120 \mathcal{M}_i . Our goal is to apply these knowledge toward learning a new MDP, denoted by \mathcal{M} . To this end,
 121 we derive a new Lipschitz upper confidence bound for \mathcal{M} , which utilizes and transfers the knowledge
 122 from past MDPs $\mathcal{M}_1, \dots, \mathcal{M}_N$, thus obtaining an improved Monte Carlo action sampling strategy
 123 that limits the tree search in \mathcal{M} to a smaller subset of sampled actions. We use $N(s, a)$ to denote
 124 the visit count of the new MDP to $(s \in S, a \in A)$, $W(s, a)$ to denote the sampled return, and thus
 125 $Q_{\mathcal{M}}^N(s, a) = W(s, a)/N(s, a)$ to denote its current Q-value estimate.

126 Our key idea in this paper is that an improved upper confidence bound for the new MDP \mathcal{M} can be
 127 obtained by (i) analyzing the Lipschitz continuity between the past and new MDPs with respect to
 128 the upper confidence bounds and (ii) taking into account the confidence and aleatory uncertainty
 129 of the learned Q-value estimates to determine to what extent the learned knowledge from each \mathcal{M}_i
 130 is pertinent. Intuitively, the more similar \mathcal{M} and \mathcal{M}_i are and the more samples (and thus higher
 131 confidence) we have in the learned Q-value estimates, the less exploration we would need to perform
 132 to solve \mathcal{M} through MCTS. Our analysis will lead to an improved upper confidence bound that guides
 133 the MCTS on the new MDP \mathcal{M} over a much smaller subset of action samples, thus significantly
 134 improving search performance. We start by introducing a definition of the distance between two
 135 given MDPs, $\mathcal{M} = \langle R, P \rangle$, $\mathcal{M}' = \langle R', P' \rangle$, with reward functions R, R' and state transitions P, P' ,
 136 respectively. We choose a positive scaling factor $\kappa > 0$ to combine the distances for transition
 137 probabilities and rewards. Proofs of all theorems and corollaries are presented in the appendix.

138 **Definition 3.1.** Given two MDPs $\mathcal{M} = \langle R, P \rangle$, $\mathcal{M}' = \langle R', P' \rangle$, and a distribution for sampling the
 139 state transitions $\mathcal{U} : \mathcal{S} \times \mathcal{A} \times \mathcal{S}' \rightarrow [0, 1]$, we define the pseudometric between the MDPs as:

$$140 d(\mathcal{M}, \mathcal{M}') = \Delta R + \kappa \cdot \Delta P = \mathbb{E}_{(s, a, s') \sim \mathcal{U}} [|R_s^a - R'^a| + \kappa |P_{ss'}^a - P'^{a'}|].$$

141 Noted that we write $d(\mathcal{M}, \mathcal{M}') = \Delta R + \kappa \cdot \Delta P$ with $\Delta_R \in [0, R_{\max}]$ and $\Delta_P \in [0, 1]$ (total-variation
 142 distance), so $d \in [0, R_{\max}] + \kappa$. The normalized advantage $\Delta_{(s, a)}^M := \frac{Q_M^*(s, a^*) - Q_M^*(s, a)}{R_{\max}/(1-\gamma)} \in [0, 1]$ κ
 143 is a constant used to remove the mismatch in units between ΔR and ΔP , the detailed derivation is
 144 given in Eq. 18.

145 Here $d(\mathcal{M}, \mathcal{M}')$ is our definition of distance between two MDPs, \mathcal{M} and \mathcal{M}' . We choose \mathcal{U} to be a
 146 uniform distribution for sampling the state transitions in this paper. In Section 4, we discuss practical
 147 algorithms to estimate the distance metric between two MDPs, from either available state-action
 148 samples using a data-driven approach or a parameterized distance using a model-based (deep learning)
 149 approach. The sampling complexity and error bounds are also analyzed.

150 Next, we prove the main result of this paper and show that the upper confidence bounds of \mathcal{M} and
 151 \mathcal{M}' are Lipschitz continuous with respect to distance $d(\mathcal{M}, \mathcal{M}')$. We obtain a new upper confidence
 152 bound for \mathcal{M} , by transferring the knowledge from the learned Q-value estimates $Q_{\mathcal{M}'}^{N'}(s, a) =$
 153 $W'(s, a)/N'(s, a)$ of MDP \mathcal{M}' . The bound also depends on the confidence of learned Q-value
 154 estimates, relating to the visit counts $N(s, a)$ and $N'(s, a)$.

155 **Theorem 3.2** (Lipschitz aUCT Rule). *Consider two MDPs \mathcal{M} and \mathcal{M}' with visit count N, N' and
 156 corresponding estimate Q-values $Q_{\mathcal{M}}^N(s, a), Q_{\mathcal{M}'}^{N'}(s, a)$, respectively. With probability at least $(1 - \delta)$
 157 for some positive $\delta > 0$, we have*

$$158 159 \left| Q_{\mathcal{M}}^N(s, a) - Q_{\mathcal{M}'}^{N'}(s, a) \right| \leq L \cdot d(\mathcal{M}, \mathcal{M}') + P(N, N') \quad (1)$$

160 161 ¹Without loss of generality, we assume that the MDPs have the same state and action spaces. Otherwise, we
 can consider the extended MDPs defined by the union of their state and action spaces.

162 where $L = 1/(1 - \gamma)$ (From Eqn 18) is a Lipschitz constant, $d(\mathcal{M}, \mathcal{M}')$ is the distance between
 163 MDPs, and $P(N, N')$ is given by
 164

$$165 \quad P(N, N') = \frac{2R_{\max}}{1 - \gamma} \sqrt{\frac{\ln(2/\delta)}{2 \cdot \min(N, N')}} \quad (2)$$

166
 167

168 In the theorem above, we show that the estimate Q-values between two MDPs are bounded by
 169 two terms, i.e., a Lipschitz continuity term depending on the distance $d(\mathcal{M}, \mathcal{M}')$ between the two
 170 environments and a confidence term depending on the number N, N' of samples used to estimate the
 171 Q-values. The Lipschitz continuity term measures how much the learned knowledge of source MDP
 172 \mathcal{M} is pertinent to the new MDP \mathcal{M}' , while the confidence terms $P(N, N')$ quantifies the sampling
 173 bias arising from statistical uncertainty due to limited sampling in MCTS. We note that as the number
 174 of samples N goes to infinity, we have $Q_{\mathcal{M}}^N(s, a) \rightarrow Q_{\mathcal{M}}^*(s, a)$ in Theorem 3.2, approaching the true
 175 Q-value $Q_{\mathcal{M}}^*(s, a)$ of the new MDP. Our theorem effectively provides an upper confidence bound
 176 for the true Q-value of the new MDP, based on knowledge transfer from the source MDP. We also
 177 note that as both numbers N, N' go to infinity, the confidence term becomes $P(N, N') \rightarrow 0$. Our
 178 theorem recovers the Lipschitz lifelong RL Lecarpentier et al. (2021b) as a special case of our results,
 179 for the true Q-values of the two MDPs.
 180

180 We apply Theorem 3.2 to MCTS-based lifelong planning with a sequence of distinct m tasks,
 181 $\mathcal{M}_1, \dots, \mathcal{M}_m$. Our goal is to obtain an improved bound on the true Q-value of the new task \mathcal{M}
 182 based on knowledge transfer. To this end, we independently apply the knowledge from each past
 183 MDP, i.e., $Q_{\mathcal{M}_i}^{N_i}(s, a) = W_i(s, a)/N_i(s, a)$, to the new MDP. By taking the minimum of these bounds
 184 and making $N \rightarrow \infty$, it provides a tightest upper bound on the true Q-value $Q_{\mathcal{M}}^*(s, a)$ of the new
 185 MDP, which is defined as our aUCT bound, as it adaptively transfers knowledge from past tasks to
 186 the new tasks in MCTS-based lifelong planning. The result is summarized in the following corollary.
 187

187 **Corollary 3.3** (aUCT bound in lifelong planning). *Given MDPs $\mathcal{M}_1, \dots, \mathcal{M}_m$, the new MDP's
 188 true Q-value is bounded by $Q_{\mathcal{M}}^*(s, a) \leq U_{\text{aUCT}}$ with probability at least $(1 - \delta)$. The aUCT bound
 189 U_{aUCT} is given by*

$$190 \quad U_{\text{aUCT}}(s, a) \triangleq \min_{1 \leq i \leq m} \left[Q_{\mathcal{M}_i}^{N_i}(s, a) + L \cdot d(\mathcal{M}, \mathcal{M}_i) + \frac{2R_{\max}}{1 - \gamma} \sqrt{\frac{\ln(2/\delta)}{2N_i(s, a)}} \right] \quad (3)$$

191
 192
 193

194 Obtaining this corollary is straightforward from Theorem 3.2 by taking $N \rightarrow \infty$ and considering
 195 the tightest bound of all knowledge transfers. In the context of MCTS-based lifelong planning, the
 196 more knowledge we have from solving past tasks, the more likely we can easily plan a new task, as
 197 the aUCT bound $U_{\text{aUCT}}(s, a)$ is taken over the minimum of all past tasks. The confidence of past
 198 knowledge, i.e., the statistical uncertainty due to sampling number N_i , also affects the knowledge
 199 transfer to the new task.
 200

201 3.2 OUR PROPOSED LiZERO ALGORITHM USING AUCT

202 We use the derived aUCT to design a highly efficient LiZero algorithm for MCTS-based lifelong planning.
 203 The LiZero algorithm transfers knowledge from past known tasks by computing $U_{\text{aUCT}}(s, a)$ in
 204 Corollary 3.3. It requires an efficient estimate of the distance $d(\mathcal{M}, \mathcal{M}_i)$ (as defined in Definition 3.1)
 205 between the source MDPs and the new (target) MDP. We will present practical algorithms for such
 206 distance estimates in the next section and present an analysis of the sampling complexity and error
 207 bounds. We will first introduce our LiZero algorithm in this section. We note that, during MCTS,
 208 direct exploration/search in the new task \mathcal{M} also produces new knowledge and leads to improved
 209 UCT bound of \mathcal{M} . Therefore, our proposed LiZero combines both knowledge transfer through
 210 $U_{\text{aUCT}}(s, a)$ and knowledge from direct exploration/search in \mathcal{M} .
 211

212 The search in our proposed LiZero algorithm is divided into three stages, repeated for a certain
 213 number of simulations. First, each simulation starts from the internal root state and finishes when
 214 the simulation reaches a leaf node. Let $Q_{\mathcal{M}}^N(s, a) = W(s, a)/N(s, a)$ be the current estimate of the
 215 new MDP and $N(s) = \sum_{a \in \mathcal{A}} N(s, a)$ be the visit count to state $s \in \mathcal{S}$. For each simulated time
 216 step, LiZero chooses an action a by maximizing a combined upper confidence bound based on aUCT,
 217 i.e., Since both terms are valid upper bounds on $Q^*(s, a)$, their minimum remains an admissible upper

216 bound, preserving optimism. We ensure sufficient exploration by standard UCB tie-breaking and a
 217 per-edge visit floor.

$$219 \quad a = \arg \max_a \min \left[\frac{W(s, a)}{N(s, a)} + C \sqrt{\frac{\ln N(s)}{N(s, a)}}, U_{\text{aUCT}}(s, a) \right]$$

221 In practice, we can also use the maximum possible return $R_{\max}/(1 - \gamma)$ as an initial value of
 222 the search. Next, at the final time step of the simulation, the reward and state are computed by a
 223 dynamics function. A new node, corresponding to the leaf state, is then added to the search tree.
 224 Finally, at the end of the simulation, the statistics along the trajectory are updated. Let G be the
 225 accumulative (discounted) reward for state-action (s, a) from the simulation. We update the statistics
 226 by: $Q_{\mathcal{M}}^{N+1}(s, a) := \frac{N(s, a) \cdot Q_{\mathcal{M}}^N(s, a) + G}{N(s, a) + 1}$, $N(s, a) := N(s, a) + 1$.

228 **No negative transfer.** By construction, LiZero always selects a^* . Therefore, if the transferred
 229 bound $U_{\text{aUCT}}(s, a)$ is loose (e.g., when tasks are dissimilar or Lipschitz regularity does not hold),
 230 the minimum simply reduces to the standard UCT confidence term, and LiZero behaves identically to
 231 vanilla UCT. In particular, Theorem 3.4 shows that the sample complexity of LiZero is never worse
 232 than that of UCT ($\Gamma \geq 1$), and equals it ($\Gamma = 1$) when no useful transfer is available.

233 Intuitively, at the start of task \mathcal{M} ’s MCTS, there are not sufficient samples available, and thus
 234 $U_{\text{aUCT}}(s, a)$ serves as a tighter upper confidence bound than that resulted from the Monte Carlo
 235 actions sampling in \mathcal{M} . As more samples are obtained during the search process, the standard UCT
 236 bound is expected to become tighter than $U_{\text{aUCT}}(s, a)$. Using both bounds will ensure efficient
 237 knowledge transfer and task-specific search. The pseudocode of LiZero is provided in Appendix A.2.

238 For the proposed LiZero algorithm, we prove that it can result in accelerated convergence in MCTS.
 239 More precisely, we analyze the sampling complexity for the learned Q-value estimate $Q_{\mathcal{M}}^N(s, a)$ to
 240 converge to the true value $Q_{\mathcal{M}}^*(s, a)$, and demonstrate a strictly positive acceleration factor, compared
 241 to the standard UCT. The results are summarized in the following theorem.

242 **Theorem 3.4.** *To ensure the convergence in a finite state-action space, $\max_{(s, a)} |Q_{\mathcal{M}}^N(s, a) -$
 243 $Q_{\mathcal{M}}^*(s, a)| \leq \epsilon$ with probability $1 - \delta$, the number of samples required by standard UCT is*

$$245 \quad \tilde{O} \left(\frac{|\mathcal{S}| \cdot |\mathcal{A}|}{(1 - \gamma)^3 \epsilon^2} \ln \frac{1}{\delta} \right), \quad (4)$$

247 while the proposed LiZero algorithm requires: $\tilde{O} \left(\frac{1}{\Gamma} \cdot \frac{|\mathcal{S}| \cdot |\mathcal{A}|}{(1 - \gamma)^3 \epsilon^2} \ln \frac{1}{\delta} \right)$. where $\Gamma > 1$ is an acceleration
 248 factor given by $\Gamma = \frac{\sum_{(s, a) \in \mathcal{S}_1 \cup \mathcal{S}_0} \frac{1}{(\Delta_{(s, a)}^{\mathcal{M}})^2}}{\sum_{(s, a) \in \mathcal{S}_1} (1) + \sum_{(s, a) \in \mathcal{S}_0} \frac{1}{(\Delta_{(s, a)}^{\mathcal{M}})^2}}$, and $\mathcal{S}_1 = \{(s, a) \mid \exists i : U_{\text{aUCT}}(s, a) <$
 251 $Q_{\mathcal{M}}^*(s, a^*)\}$ is a state-action set where U_{aUCT} of action a is lower than the optimal return of a^* in
 252 state s ; and $\Delta_{(s, a)}^{\mathcal{M}} \propto [Q_{\mathcal{M}}^*(s, a^*) - Q_{\mathcal{M}}^*(s, a)]$ is a normalized advantage in the range of $[0, 1]$.

254 The theorem shows that LiZero achieves a strictly improved acceleration $\Gamma > 1$ with a reduced
 255 sampling complexity (by $1/\Gamma$), in terms of ensuring convergence to the optimal estimates, i.e.,
 256 $\max_{(s, a)} |Q_{\mathcal{M}}^N(s, a) - Q_{\mathcal{M}}^*(s, a)| \leq \epsilon$ with probability $1 - \delta$. Since the normalized advantage $\Delta_{(s, a)}^{\mathcal{M}}$
 257 is in $[0, 1]$, we have $1/\Delta_{(s, a)}^{\mathcal{M}} \geq 1$. It follows that $\Gamma > 1$ whenever $\mathcal{S}_1 \neq \emptyset$; when $\mathcal{S}_1 = \emptyset$, LiZero
 258 reduces to UCT and $\Gamma = 1$. More precisely, LiZero achieves higher acceleration when (i) our aUCT
 259 makes more actions a less favorable, as $U_{\text{aUCT}}(s, a) < Q_{\mathcal{M}}^*(s, a^*)$ implies that the sub-optimality
 260 of action a in s can be more easily determined due to aUCT; or (ii) aUCT helps establish tighter
 261 bounds in cases with a smaller advantage, which naturally requires more samples to distinguish the
 262 optimal actions – since Γ increases as the normalized advantage becomes smaller for $(s, a) \in \mathcal{S}_1$,
 263 while being larger for $(s, a) \in \mathcal{S}_0$. These explain LiZero’s ability to achieve much higher acceleration
 264 and lower sampling complexity, resulted from significantly reduced search spaces. We will evaluate
 265 this acceleration/speedup through experiments in Section 5.

266 4 ESTIMATING AUCT IN PRACTICE

267 To deploy LiZero in practice, we propose two approaches for estimating aUCT, and in particular,
 268 the distance $d_{\mathcal{M}, \mathcal{M}_i}$ between two MDPS. Our first approach leverages trajectory samples drawn

270 from MCTS policies by modeling a sequence of distinct policies as a filtration – i.e., an increasing
 271 sequence of σ -algebra, while our second approach learns neural network approximations of the
 272 MDPs. Analysis of sampling complexity and error bounds are provided as theorems in this section.
 273

274 **Sample-based Distance Estimate.** During MCTS, transition samples are collected from the search
 275 to train a search policy π . It is easy to see that we can leverage these transition samples to estimate
 276 distance $d(\mathcal{M}, \mathcal{M}')$ between two MDPs, as long as we address the bias arising from gap between
 277 search policy π and desired sampling distribution \mathcal{U} in the distance definition $d(\mathcal{M}, \mathcal{M}')$. It also
 278 allows us to obtain a consistent estimate of MDP distance, without depending on the search policy
 279 that is updated during training. We note that this bias can be addressed by importance sampling.

280 Let $\Delta X(s, a) = \Delta R_s^a + \kappa \Delta P_s^a$ be the distance metric for a given state-action pair (s, a) . We can
 281 rewrite the distance as $d(\mathcal{M}, \mathcal{M}') = \mathbb{E}_{(s, a) \sim \mathcal{U}} [\Delta X(s, a)]$. We denote $p_{\mathcal{U}}(s, a)$ as the probability (or
 282 density) of sampling (s, a) according to distribution \mathcal{U} . Importance sampling implies:

$$\mathbb{E}_{(s, a) \sim \mathcal{U}} [\Delta X(s, a)] = \mathbb{E}_{(s, a) \sim \pi} \left[\frac{p_{\mathcal{U}}(s, a)}{\pi(s, a)} \cdot \Delta X(s, a) \right], \quad (5)$$

286 which can be readily computed from the collected transition samples, following the search policy
 287 $\pi(s, a)$. Therefore, for a given set of samples $\{(s_i, a_i), \forall i = 1, \dots, n\}$ collected from a search policy
 288 $\pi(s, a)$, we can estimate the distance by the empirical mean:

$$\hat{d}_1 = \frac{1}{n} \sum_{i=1}^n w_i \Delta X(s_i, a_i), \text{ with } w_i = \frac{\mathcal{U}(s_i, a_i)}{\pi(s_i, a_i)} \quad (6)$$

292 where w_i is the importance sampling weight.
 293

294 As long as the state-action pairs with $\pi(s, a) > 0$ cover the support of \mathcal{U} , this estimator satisfies
 295 $\mathbb{E}[\hat{d}_1] = d(\mathcal{M}, \mathcal{M}')$, meaning it is unbiased. Let α be the "coverage" of policy $\pi(s, a)$, i.e.
 296 $\pi(s, a) \geq \alpha > 0$, and let $p_{\mathcal{U}}^{\max}$ be the maximum desired sampling probability. We summarize
 297 this result in the following theorem and state the sampling complexity for estimator \hat{d}_1 to ϵ -converge
 298 to $d(\mathcal{M}, \mathcal{M}')$.

299 In our tabular gridworld experiments, both the state and action spaces are finite. We instantiate the
 300 reference distribution \mathcal{U} in Definition 3.1 as the uniform distribution over state-action pairs, $\mathcal{U}(s, a) =$
 301 $\frac{1}{|\mathcal{S}| |\mathcal{A}|}$. The importance weights in LiZero-P are then given by $w_i = \frac{\mathcal{U}(s_i, a_i)}{\pi(s_i, a_i)}$, where π denotes the
 302 empirical tree policy estimated from visit counts under UCT-style exploration. In the finite gridworlds,
 303 every action at a visited state has a strictly positive lower bound on $\pi(s, a)$, so the weights $\{w_i\}$ are
 304 almost surely bounded and we observe no variance explosion in practice. For larger or continuous
 305 domains, standard techniques such as self-normalized importance sampling and weight clipping can
 306 be incorporated without changing the theoretical analysis.

307 **Theorem 4.1** (Sampling Complexity under Stationarity). *Assume that for any (s, a) , the reward
 308 plus transition difference is bounded, i.e., $\Delta X(s, a) \in [0, b]$, and that there exists α such that
 309 $\pi(s, a) \geq \alpha > 0$. When n independent samples are used to estimate \hat{d}_1 , we have*

$$\Pr\{|\hat{d}_1 - d(\mathcal{M}, \mathcal{M}')| \leq \epsilon\} \geq 1 - \delta \quad (7)$$

313 for any $\delta \in (0, 1)$, if the number of samples satisfy $n \geq \frac{1}{2\epsilon^2} b^2 \left(\frac{p_{\mathcal{U}}^{\max}}{\alpha} \right)^2 \cdot \ln \left(\frac{2}{\delta} \right)$. Thus, we obtain a
 314 convergence guarantee in the sense of arbitrarily high probability $1 - \delta$ and arbitrarily small error ϵ ,
 315 for estimating $d(\mathcal{M}, \mathcal{M}')$ using \hat{d}_1 . \hat{d}_1 is unbiased and ensures convergence to the true distance as
 316 the number of samples is sufficiently large.

318 We note that in many practical settings, the search policy π would not stick to a stationary distribution.
 319 In contrast, it is continuously updated in each iteration, resulting in a sequence of distinct policies
 320 over time, i.e., $\pi_1, \pi_2, \dots, \pi_k$. Thus, the transition samples (s_k, a_k) 's we obtain at each step k for
 321 estimating the distance $d(\mathcal{M}, \mathcal{M}')$ are indeed drawn from a different π_k . We cannot assume that the
 322 samples follow a stationary distribution (nor that $\{\Delta X_k^w\}$ are i.i.d.) in importance sampling. we
 323 model the sequence of distinct policy updates as a filtration – i.e., an increasing sequence of σ -algebra.
 In particular, we make the following assumption: at the k -th sampling step, the environment is

324 forcibly reset to a predetermined policy π_k or independently draws a state from an external memory.
 325 This assumption is reasonable, in many episodic learning scenarios, the environment is inherently
 326 divided into episodes: at the beginning of each episode, the state is reset to some initial distribution
 327 (e.g., the opening state in Atari games). This naturally results in the “reset” assumption.

328 In this setup, the policy π_k at step k is determined by information at step $k-1$ or earlier. Consequently,
 329 once π_k is fixed, the distribution (marginal) of $\Delta X_k^w = \frac{p_{\mathcal{U}}(s_k, a_k)}{\pi_k(s_k, a_k)} \Delta X(s_k, a_k)$ is also fixed. Therefore,
 330 we can establish the filtration $\{\mathcal{F}_k, k = 1, 2, \dots\}$ as follows:

$$\mathcal{F}_{k-1} = \sigma\{\pi_1, \dots, \pi_k, (s_1, a_1), \dots, (s_{k-1}, a_{k-1})\}, \quad (8)$$

331 where $\sigma\{\cdot\}$ denotes the smallest σ -algebra generated by the random elements. Thus, we obtain:

$$\mathbb{E}[\Delta X_k | \mathcal{F}_{k-1}] = \mathbb{E}_{(s_k, a_k) \sim \pi_k} \left[\frac{p_{\mathcal{U}}(s_k, a_k)}{\pi_k(s_k, a_k)} \cdot \Delta X(s_k, a_k) \right] = \mathbb{E}_{(s_k, a_k) \sim \mathcal{U}} [\Delta X(s, a)] = d(\mathcal{M}, \mathcal{M}') \quad (9)$$

332 This allows us to obtain another empirical estimator \hat{d}_2 using the filtration model. We analyze the
 333 sampling complexity of \hat{d}_2 and summarise the results in the following theorem.

334 **Theorem 4.2** (Sampling Complexity under task-to-task variation). *Under the same conditions as*
 335 *Theorem 4.1 when n independent samples are used to estimate \hat{d}_2 , we have $\Pr\{|\hat{d}_2 - d(\mathcal{M}, \mathcal{M}')| \leq$*
 336 *$\epsilon\} \geq 1 - \delta$ for any $\delta \in (0, 1)$, if the number of samples satisfy $n \geq \frac{2}{\epsilon^2} b^2 \left(\frac{p_{\mathcal{U}}^{\max}}{\alpha}\right)^2 \cdot \ln\left(\frac{2}{\delta}\right)$.*

337 It implies that more samples are needed, considering the task-to-task variation of the policy update
 338 process for the distance estimate. We approximate the filtration by resetting episodes and re-sampling
 339 initial states from a replay buffer at task boundaries.

340 **NN-based Distance Estimate.** We propose an alternative approach to first approximate the dy-
 341 namics of MDPs \mathcal{M} and \mathcal{M}' using two neural networks and then estimate $d(\mathcal{M}, \mathcal{M}')$ based on the
 342 parameterized distance between the neural networks. To this end, we need to establish a bound
 343 on $d(\mathcal{M}, \mathcal{M}')$ using the distance between their neural network parameters. We use a neural net-
 344 work $\Psi_{\phi} : \mathcal{S} \times \mathcal{A} \rightarrow \Delta(\mathcal{S})$ to model the MDP dynamics. Many model-based learning algorithms,
 345 such as PILCO Deisenroth & Rasmussen (2011), MBPO Janner et al. (2019), PETS Chua et al.
 346 (2018), MuZero Schrittwieser et al. (2020b), can be employed to learn the models of \mathcal{M} and \mathcal{M}' . Let
 347 ϕ be the neural network parameters of MDP \mathcal{M} and ϕ' be the neural network parameters of MDP
 348 \mathcal{M}' . We define a distance in the parameter space: $\hat{d}_{para} = \rho(\phi, \phi') \geq 0$, where ρ is a distance or
 349 divergence measure in the parameter space, such as the ℓ_2 -norm or certain kernel distances. Intuitively,
 350 if ϕ and ϕ' are very close, the two neural networks are similar in fitting the dynamics of the respective
 351 MDPs. It suggests that the two MDPs should have a small distance. To provide a more rigorous
 352 characterization of this concept, we present the following theorem, which demonstrates that under
 353 proper assumptions, the distance \hat{d}_{para} based on neural network parameters can serve as an upper
 354 bound for the desired $d(\mathcal{M}, \mathcal{M}')$. Let $\kappa = R_{\max} \gamma / (1 - \gamma)$ be a constant.

355 **Theorem 4.3.** *If the neural networks modeling \mathcal{M} and \mathcal{M}' satisfy the Lipschitz condition, i.e., there*
 356 *exists a constant $L > 0$ such that $\forall (s, a), \|\Psi_{\phi}(s, a) - \Psi_{\phi'}(s, a)\|_1 \leq L \cdot \rho(\phi, \phi')$, then we have:*
 357 $d(\mathcal{M}, \mathcal{M}') \leq (1 + \kappa) L \hat{d}_{para}$.

358 The theorem indicates that by learning neural networks to model the MDP dynamics, we can estimate
 359 the distance $d(\mathcal{M}, \mathcal{M}')$ by estimating the distance between the neural network parameters. This
 360 parameterized distance can be computed for event continuous action and state spaces.

361 5 EVALUATIONS

362 Our experiments evaluate LiZero on a series of ten learning tasks with varying transition probabilities
 363 and rewards. We demonstrate LiZero’s ability to transfer past knowledge in MCTS-based planning,
 364 resulting in significant convergence speedup (3~4x) and early reward improvement (about 31%
 365 average improvement during the first half of learning process) in lifelong planning problems. All
 366 experiments are conducted on a Linux machine with AMD EPYC 7513 32-Core Processor CPU and
 367 an NVIDIA RTX A6000 GPU, implemented in python3. All source codes are made available in the
 368 supplementary material.

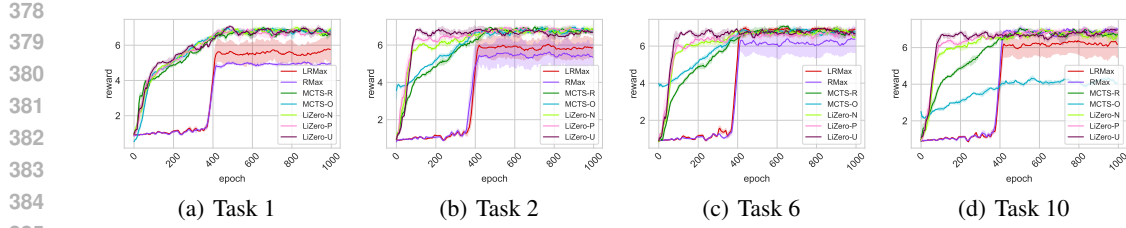


Figure 1: Comparing LiZero with MCTS and lifelong RL baselines. We demonstrate the convergence of different algorithms on representative Tasks 1, 2, 6, and 10, in a sequence of distinct ten tasks. In Task 1, since no prior knowledge is yet available, our LiZero and other MCTS baselines show similar convergence speeds and optimal rewards. From Task 2 to Task 10, as more knowledge from past tasks gets transferred to the new task by LiZero, it outperforms all baselines with more significantly improved convergence speed. In Task 10 with maximum past knowledge, LiZero demonstrates the largest improvement in convergence speed and optimal reward.

Name	Task1	Task2	Task3	Task4	Task5	Task6	Task7	Task8	Task9	Task10	Total
LiZero-U	4.83±0.05	5.98±0.10	5.99±0.07	5.94±0.05	6.08±0.07	6.05±0.16	6.01±0.11	6.03±0.05	6.04±0.04	6.03±0.09	58.98
LiZero-P	4.65±0.06	5.89±0.11	5.90±0.12	5.90±0.03	5.62±0.19	5.68±0.22	5.76±0.12	5.87±0.03	5.78±0.06	5.79±0.20	56.84
LiZero-N	4.64±0.08	5.56±0.07	5.56±0.07	5.52±0.05	5.52±0.08	5.48±0.06	5.50±0.09	5.45±0.06	5.50±0.06	5.48±0.05	54.21
MCTS-R	4.51±0.07	4.43±0.08	4.32±0.11	4.24±0.05	4.18±0.07	4.24±0.10	4.25±0.03	4.47±0.06	4.34±0.03	4.39±0.08	43.37
MCTS-O	4.52±0.06	4.87±0.08	4.57±0.04	4.16±0.03	4.78±0.05	4.91±0.06	4.04±0.03	3.70±0.05	3.02±0.07	2.96±0.06	41.53
pUCT	4.66±0.04	4.71±0.06	4.69±0.13	4.77±0.09	4.74±0.04	4.87±0.05	4.94±0.06	4.72±0.05	4.86±0.07	4.77±0.03	47.73
RMax	1.02±0.02	1.05±0.01	1.01±0.02	1.03±0.01	1.04±0.01	1.05±0.01	1.03±0.03	1.04±0.02	1.03±0.02	1.03±0.01	10.33
LRMax	1.05±0.01	1.05±0.02	1.04±0.02	1.06±0.03	1.05±0.01	1.06±0.02	1.04±0.01	1.06±0.03	1.05±0.01	1.04±0.01	10.50

Table 1: The table summarizes the rewards and standard deviations obtained in sequential tasks. It shows that LiZero achieves about 31% early reward improvement on average, compared with MCTS baselines (including two versions of MCTS with UCT Winands (2024); Kocsis & Szepesvari (2006); Cheng et al. and one with pUCT similar to MuZero Schrittwieser et al. (2020a)) and lifelong RL baselines (including RMax Brafman & Tennenholz (2002) and LRMax Lecarpentier et al. (2021a)). MCTS-R and MCTS-O demonstrate similar level of performance, both better than lifelong RL and slightly below pUCT. LiZero algorithms outperform MCTS baselines by about 31% early reward improvement on average. With more accurate distance estimates – i.e., from Lizero-N to LiZero-P and LiZero-U – we observe further improvement due to better knowledge transfer that comes with more accurate aUCT.

In the evaluation, we consider some state-of-the-art baselines using MCTS and lifelong RL. In particular, we consider two versions of MCTS algorithms that leverage UCT Winands (2024); Kocsis & Szepesvari (2006); Cheng et al.: MCTS-R denotes a version that restarts the search from scratch for each new task, and MCTS-O denotes a version that is oblivious to the sequence of distinct task dynamics and continues to build upon the search tree from the past. We also consider state-of-the-art MCTS using pUCT, similar to MuZero and related algorithms Schrittwieser et al. (2020a). We have two lifelong RL algorithms: RMax Brafman & Tennenholz (2002) and LRMax Lecarpentier et al. (2021a), which exploits a similar Lipschitz continuity in RL but does not consider MCTS using upper confidence bounds. We evaluated three versions of LiZero using different methods to estimate aUCT by computing task distances, as presented in Section 4. LiZero-U employs a direct distance estimator \hat{d}_2 using samples following the search policy; and LiZero-N is the neural-network based estimator \hat{d}_{para} using parameter distances.

The experimental environment we used is a variation of the "tight" task by Abel et al. Abel et al. (2018). It generates a sequence of ten learning tasks. Each task consists of a 25×25 grid world, with the initial state located at the center, and four possible actions: up, down, left, and right. The three

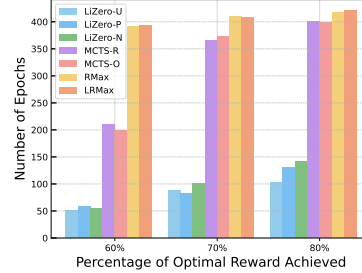
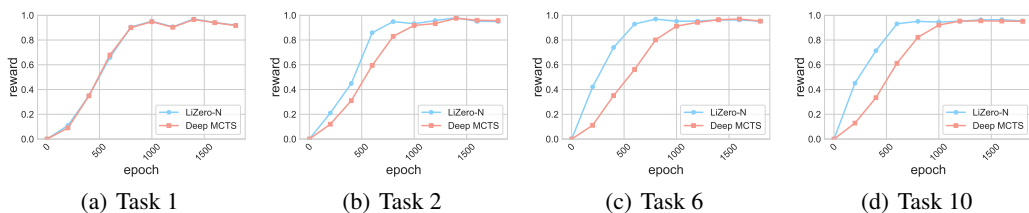


Figure 2: LiZero shows a comfortable speedup of 3~4x, compared with MCTS and lifelong RL baselines, to achieve the same level of optimal rewards with higher sample efficiency.

432 cells in the top-right corner and one cell in the bottom-left corner are designated as goal cells. For
 433 each task, the reward for the goal cells is randomly chosen from the range $[0.9, 1]$. The remaining
 434 cells will randomly generate interference rewards within the range $[0, 0.1]$. Its state transition matrix
 435 selects its own slip probability (acting differently from the chosen one) within the range $[0, 0.1]$. This
 436 ensures that the sequence of tasks has varying reward and transition probabilities. Each task is for
 437 1,000 epochs. These operations are repeated multiple times to narrow the confidence interval.

438 Figure 1 shows the convergence of different algorithms on representative Tasks 1, 2, 6, and 10, in a
 439 sequence of ten distinct tasks. As tasks are drawn sequentially, LiZero-U, LiZero-P, and LiZero-N
 440 algorithms converge more rapidly than the MCTS and lifelong RL baselines. This speedup becomes
 441 evident as early as the second task (Task 2) – while similar convergences are observed in Task 1 as no
 442 prior knowledge is yet available. From Task 2 to Task 10, as more knowledge from past tasks gets
 443 transferred to the new task by LiZero, it outperforms all baselines in significantly more improved
 444 convergence speed. In Task 10 with maximum past knowledge, LiZero outperforms all baselines in
 445 convergence speed and optimal reward. MCTS-O (which is oblivious to changing task dynamics)
 446 exhibits worse performance than MCTS-R (which restarts from scratch).

447 In Table 1, we summarize the average rewards (and their standard deviations) obtained in sequential
 448 tasks by different algorithms during their first 500 epochs (i.e., first half of the learning process).
 449 LiZero algorithms achieves about 31% early reward improvement on average. As for MCTS baselines
 450 with UCT, MCTS-R shows similar reward across different tasks, while MCTS-O demonstrates higher
 451 volatility – due to its reliance on how task dynamics evolve. pUCT achieves higher performance
 452 due to the use of improved probabilistic UCT similar to MuZero. All MCTS baselines show better
 453 results than lifelong RL algorithms (i.e., RMax and LRMax), which are known to be less sample
 454 efficient and require more epochs for exploration/exploitation. With more accurate distance estimates
 455 – i.e., from Lizer-N to LiZero-P and to LiZero-U – we observe further improved results due to better
 456 knowledge transfer that comes with more accurate aUCT calculations.



457
 458 Figure 3: Performance of LiZero-N and Deep MCTS on a continuous-state MuJoCo Point Maze
 459 sequence. Each panel shows the normalized return versus planning epochs for Tasks 1, 2, 6, and 10. On
 460 the first task LiZero-N performs similarly to Deep MCTS, while on later tasks it converges faster and
 461 achieves higher early returns, demonstrating that aUCT-based transfer remains effective in continuous
 462 MDPs and that its benefits grow as more tasks are learned.

463
 464 To demonstrate that the proposed aUCT transfer is not limited to discrete gridworlds, we further
 465 evaluate LiZero-N in a continuous state-space environment, the MuJoCo Point Maze. The environ-
 466 ment consists of a point mass with two degrees of freedom (x, y) that is force-actuated in Cartesian
 467 coordinates and must reach a target goal position inside a closed maze. We construct a sequence of 10
 468 tasks by randomly modifying the maze parameters and goal locations. Each task is solved by running
 469 MCTS for 2,000 planning epochs. We compare LiZero-N with the same Deep MCTS baseline used
 470 in the gridworld experiments. Figure 3 reports the normalized returns averaged over multiple runs.

471 To evaluate the speedup of LiZero, Figure 2 shows the average number of epochs needed by different
 472 algorithms to achieve 60%, 70%, and 80% of the optimal reward, respectively. We note that LiZero
 473 shows a comfortable speedup of 3~4x, compared to MCTS and lifelong RL baselines, while RL
 474 baselines are much less sample-efficient than MCTS-based planning, in general. We do not go beyond
 475 80% in this plot since some baselines are never able to achieve more than 80% of the optimal reward
 476 that LiZero obtains. The results validate the acceleration as characterized by Γ in Theorem 3.4.

477
 478 **Ablation Study.** Our ablation study considers the impact of distance estimator on performance.
 479 Figure 4 shows the distance estimators in LiZero-U, LiZero-P, and LiZero-N (each with decreasing
 480 accuracy) across the sequence of tasks, while for the purpose of ablation study, MCTS-R can be
 481 viewed as an algorithm without distance estimator. Comparing the performance of these algorithms in

Table 1 and Figure 2, we see that the superior performance of LiZero is indeed resulted from the use of aUCT in MCTS – The tighter aUCT bounds we use, the higher performance we can achieve. Using no distance estimator and thus only UCT (in MCTS-R) leads to the lowest performance. Further, as tasks are drawn, the distance estimates decrease quickly, and by the third task, it is already very small, implying accurate aUCT calculation for knowledge transfer.

6 CONCLUSIONS

We study theoretically the transfer of past knowledge in MCTS-based lifelong planning and develop a novel aUCT rule, depending on both Lipschitz continuity between tasks and the confidence of knowledge in Monte Carlo action sampling. The proposed aUCT is proven to significantly accelerate MCTS and enable a new lifelong MCTS algorithm: LiZero. We present efficient methods for online estimation of aUCT and analyze the sampling complexity and error bounds. LiZero is evaluated on a sequence of distinct tasks with varying transition probabilities and rewards. It outperforms MCTS and lifelong RL baselines with 3~4x speed-up and about 31% higher early reward.

Limitations: The derivation of Theorem 3.2 considers varying transition probabilities and rewards, while assuming the same state and action spaces. In this case, we could consider the union of state and action spaces, but better approaches may be needed. Further, our acceleration analysis *advantage gap* to compute the acceleration factor leading to underestimation of acceleration factor

REFERENCES

David Abel, Yuu Jinnai, Sophie Yue Guo, George Konidaris, and Michael Littman. Policy and value transfer in lifelong reinforcement learning. In *International Conference on Machine Learning*, pp. 20–29. PMLR, 2018.

David Auger, Adrien Couetoux, and Olivier Teytaud. Continuous upper confidence trees with polynomial exploration–consistency. In *Machine Learning and Knowledge Discovery in Databases: European Conference, ECML PKDD 2013, Prague, Czech Republic, September 23–27, 2013, Proceedings, Part I* 13, pp. 194–209. Springer, 2013.

Ronen I Brafman and Moshe Tennenholtz. R-max-a general polynomial time algorithm for near-optimal reinforcement learning. *Journal of Machine Learning Research*, 3(Oct):213–231, 2002.

Scott Cheng, Mahmut Kandemir, and Ding-Yong Hong. Speculative monte-carlo tree search. In *The Thirty-eighth Annual Conference on Neural Information Processing Systems*.

Kurtland Chua, Roberto Calandra, Rowan McAllister, and Sergey Levine. Deep reinforcement learning in a handful of trials using probabilistic dynamics models. *Advances in neural information processing systems*, 31, 2018.

Rémi Coulom. Efficient selectivity and backup operators in monte-carlo tree search. In *International conference on computers and games*, pp. 72–83. Springer, 2006.

Felipe Leno Da Silva, Matthew E Taylor, and Anna Helena Reali Costa. Autonomously reusing knowledge in multiagent reinforcement learning. In *IJCAI*, pp. 5487–5493, 2018.

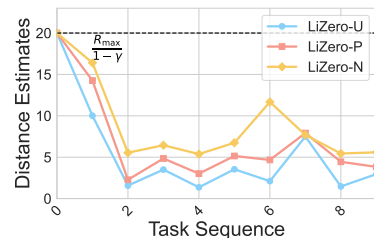


Figure 4: Our ablation study comparing different distance estimators in LiZero-U, LiZero-P, and LiZero-N, while MCTS-R can be viewed as a baseline without distance estimator. The relevant performance of these algorithms are provided in Table 1 and Figure 2 and thus not repeated here. The superior performance of LiZero is indeed resulted from the use of aUCT in MCTS. The tighter aUCT bounds, the higher performance we can obtain.

requires that the optimal Q-function has a bounded Γ . This bound may be loose for practical problems, Γ .

540 Marc Deisenroth and Carl E Rasmussen. Pilco: A model-based and data-efficient approach to policy
 541 search. In *Proceedings of the 28th International Conference on machine learning (ICML-11)*, pp.
 542 465–472, 2011.

543 Haotian Fu, Shangqun Yu, Michael Littman, and George Konidaris. Model-based lifelong reinforce-
 544 ment learning with bayesian exploration. *Advances in Neural Information Processing Systems*, 35:
 545 32369–32382, 2022.

546 Dani Goldberg and Maja J Matarić. Maximizing reward in a non-stationary mobile robot environment.
 547 *Autonomous Agents and Multi-Agent Systems*, 6:287–316, 2003.

548 Majd Hawasly and Subramanian Ramamoorthy. Lifelong learning of structure in the space of policies.
 549 In *2013 AAAI Spring Symposium Series*, 2013.

550 Pablo Hernandez-Leal, Michael Kaisers, Tim Baarslag, and Enrique Munoz De Cote. A sur-
 551vey of learning in multiagent environments: Dealing with non-stationarity. *arXiv preprint*
 552 *arXiv:1707.09183*, 2017.

553 Michael Janner, Justin Fu, Marvin Zhang, and Sergey Levine. When to trust your model: Model-based
 554 policy optimization. *Advances in neural information processing systems*, 32, 2019.

555 Levente Kocsis and Csaba Szepesvári. Bandit based monte-carlo planning. In *European conference*
 556 *on machine learning*, pp. 282–293. Springer, 2006.

557 Erwan Lecarpentier, David Abel, Kavosh Asadi, Yuu Jinnai, Emmanuel Rachelson, and Michael L
 558 Littman. Lipschitz lifelong reinforcement learning. In *Proceedings of the AAAI Conference on*
 559 *Artificial Intelligence*, volume 35, pp. 8270–8278, 2021a.

560 Erwan Lecarpentier, David Abel, Kavosh Asadi, Yuu Jinnai, Emmanuel Rachelson, and Michael L.
 561 Littman. Lipschitz lifelong reinforcement learning, 2021b. URL <https://arxiv.org/abs/2001.05411>.

562 Qihan Liu, Jianing Ye, Xiaoteng Ma, Jun Yang, Bin Liang, and Chongjie Zhang. Efficient multi-agent
 563 reinforcement learning by planning. *arXiv preprint arXiv:2405.11778*, 2024.

564 Kevin Lu, Aditya Grover, Pieter Abbeel, and Igor Mordatch. Reset-free lifelong learning with
 565 skill-space planning. *arXiv preprint arXiv:2012.03548*, 2020.

566 Kiminori Matsuzaki. Empirical analysis of puct algorithm with evaluation functions of different
 567 quality. In *2018 Conference on Technologies and Applications of Artificial Intelligence (TAAI)*, pp.
 568 142–147. IEEE, 2018.

569 Hossein Pourshamsaei and Amin Nobakhti. Predictive reinforcement learning in non-stationary
 570 environments using weighted mixture policy. *Applied Soft Computing*, 153:111305, 2024.

571 Julian Schrittwieser, Ioannis Antonoglou, Thomas Hubert, Karen Simonyan, Laurent Sifre, Simon
 572 Schmitt, Arthur Guez, Edward Lockhart, Demis Hassabis, Thore Graepel, Timothy Lillicrap, and
 573 David Silver. Mastering atari, go, chess and shogi by planning with a learned model. *Nature*, 588
 574 (7839):604–609, December 2020a. ISSN 1476-4687. doi: 10.1038/s41586-020-03051-4. URL
 575 <http://dx.doi.org/10.1038/s41586-020-03051-4>.

576 Julian Schrittwieser, Ioannis Antonoglou, Thomas Hubert, Karen Simonyan, Laurent Sifre, Simon
 577 Schmitt, Arthur Guez, Edward Lockhart, Demis Hassabis, Thore Graepel, et al. Mastering atari,
 578 go, chess and shogi by planning with a learned model. *Nature*, 588(7839):604–609, 2020b.

579 David Silver, Aja Huang, Chris J Maddison, Arthur Guez, Laurent Sifre, George Van Den Driessche,
 580 Julian Schrittwieser, Ioannis Antonoglou, Veda Panneershelvam, Marc Lanctot, et al. Mastering
 581 the game of go with deep neural networks and tree search. *nature*, 529(7587):484–489, 2016.

582 David Silver, Thomas Hubert, Julian Schrittwieser, Ioannis Antonoglou, Matthew Lai, Arthur Guez,
 583 Marc Lanctot, Laurent Sifre, Dharshan Kumaran, Thore Graepel, et al. Mastering chess and shogi
 584 by self-play with a general reinforcement learning algorithm. *arXiv preprint arXiv:1712.01815*,
 585 2017.

594 Mark HM Winands. Monte-carlo tree search. In *Encyclopedia of computer graphics and games*, pp.
595 1179–1184. Springer, 2024.
596

597 Annie Xie, James Harrison, and Chelsea Finn. Deep reinforcement learning amidst lifelong non-
598 stationarity. *arXiv preprint arXiv:2006.10701*, 2020.
599
600
601
602
603
604
605
606
607
608
609
610
611
612
613
614
615
616
617
618
619
620
621
622
623
624
625
626
627
628
629
630
631
632
633
634
635
636
637
638
639
640
641
642
643
644
645
646
647

648 A APPENDIX / SUPPLEMENTAL MATERIAL
649650 THE USE OF LARGE LANGUAGE MODELS (LLMs)
651652 The authors did not use Large Language Models for research ideation, derivations, proofs, ex-
653 perimental design, data analysis, or writing of the manuscript. No LLM contributed content that would
654 qualify as authorship or a significant contribution under the conference policy.
655656 IMPACT STATEMENT
657658 This paper proposes a novel framework for applying Monte Carlo Tree Search (MCTS) in lifelong
659 learning settings, addressing the challenges posed by non-stationary environments and dynamic game
660 dynamics. By introducing the adaptive Upper Confidence Bound for Trees (aUCT) and leveraging
661 insights from previous MDPs (Markov Decision Processes), our work significantly enhances the
662 efficiency and adaptability of decision-making algorithms across evolving tasks.
663664 The broader societal implications of this research include its potential to improve AI applications in
665 robotics, automated systems, and other domains requiring dynamic decision-making under uncertainty.
666 For instance, this framework could be used in autonomous systems to adaptively respond to changing
667 environments, thereby improving safety and reliability. At the same time, it is crucial to acknowledge
668 and mitigate potential risks, such as unintended biases or over-reliance on prior knowledge that may
669 not fully represent novel situations.670 Ethical considerations for this work focus on its use in high-stakes applications, such as healthcare,
671 finance, or defense, where decision-making under uncertainty could have significant consequences.
672 Developers and practitioners should implement safeguards to ensure responsible deployment, includ-
673 ing comprehensive testing in diverse scenarios and establishing clear boundaries for its use.674 By advancing the state of the art in continual learning and decision-making, this research contributes
675 to the development of more adaptable and intelligent AI systems while highlighting the importance
676 of ethical and responsible innovation in AI technologies.
677678 A.1 PROOF OF THEOREM 3.2
679680 *Proof.* Proof of Theorem 3.2 Since in the MCTS UCB algorithm, the estimated Q-values are obtained
681 through multiple simulations, we need to analyze how the differences in simulation results between
682 two MDPs affect the estimated Q-values.683 However, due to the randomness involved in the simulation process of the two MDPs:
684685

- **Transition randomness:** Due to different transition probabilities, the two MDPs may move
686 to different next states even when starting from the same state and action.
- **Action selection randomness:** When using the UCB algorithm, action selection depends
687 on the current statistical information, which in turn relies on the past simulation results.

688689 The randomness mentioned above makes it impossible for us to compare two independent random
690 simulation processes directly.
691692 To eliminate the impact of randomness, we need to construct a coupled simulation process for the
693 two MDPs in the same probability space, allowing for a direct comparison between them. Then we
694 will incorporate the additional errors caused by randomness into the analysis as error terms. For this
695 purpose, we present the following assumptions.
696697 **Assumption A.1.** Let us temporarily assume that the actions selected in each simulation are the same
698 for the two MDPs.
699700

- **Initial action consistency:** The simulation starts from the same states
- **Action selection consistency:** The same action a is chosen in each state.

701

702 Note: This is a strong assumption and may not hold in practice. We will discuss its impact later.
 703
 704 Thus, we can obtain the difference in cumulative rewards between the two MDPs in a single simulation
 705 as:

706

$$\Delta G = G_M - G_{M'} = \sum_{t=0}^T \gamma^t (R(s_t^M, a_t) - R'(s_t^{M'}, a_t)) \quad (10)$$

707

710 Where s_t^M and $s_t^{M'}$ are the states of the two MDPs at step t , and a_t is the action selected at step t .
 711

712 So we can get

713

$$\left| Q_M^N(s, a) - Q_{M'}^{N'}(s, a) \right| = \left| \frac{1}{N} \sum_{i=1}^N G_{M,i} - \frac{1}{N'} \sum_{i=1}^{N'} G_{M,i} \right| \leq \bar{\Delta}G = \left| \frac{1}{n} \sum_{i=1}^n \Delta G_i \right| \quad (11)$$

714

715 where $n = \min\{N, N'\}$ To estimate the expectation and variance of ΔG , we need to analyze how
 716 the differences in the state sequences affect the cumulative rewards.
 717

718 We present several settings for the state differences.
 719

720

- 721 • **Probability of state difference:** At each time step t , the probability that the states of the
 722 two MDPs differ is denoted as p_t .
- 723 • **Initial state is the same:** $p_0 = 0$.
- 724 • **State difference propagation:** Due to differences in transition probabilities, state differ-
 725 ences may accumulate in subsequent time steps.

726

727 Since the probability of state differences occurring at each step is difficult to calculate precisely, we
 728 can use the total variation distance to estimate the probability of transitioning to different states. We
 729 present the definition of the total variation distance between the transition probabilities of the two
 730 MDPs and a recursive method for calculating the probability of state differences.
 731

732

733 **Definition A.2.** Under action a_t , starting from state s_t , the total variation distance between the
 734 transition probabilities of the two MDPs is:
 735

736

$$D_{TV}(P, P') = \frac{1}{2} \sum_{s'} |P(s'|s_t, a_t) - P'(s'|s_t, a_t)| \quad (12)$$

737

738 Thus, starting from the same state s_t and action a_t , the probability that the two MDPs transition to
 739 different next states is at most $D_{TV}(P, P') \leq \frac{\Delta P}{2}$.
 740

741 Thus, the probability of state differences occurring can be recursively expressed as:
 742

743

$$p_{t+1} \leq p_t + (1 - p_t) \cdot D_{TV}(P, P') \leq p_t + \frac{\Delta P}{2} \quad (13)$$

744

745 So

746

$$p_t \leq t \cdot \frac{\Delta P}{2} \quad (14)$$

747

756 Thus, at each time step t , the expected difference in cumulative rewards is:
 757

$$\begin{aligned}
 758 \mathbb{E}[|\Delta G|] &= \mathbb{E}\left[\sum_{t=0}^T \gamma^t (R(s_t^M, a_t) - R'(s_t^{M'}, a_t))\right] \\
 759 &= \sum_{t=0}^T \gamma^t \left(\underbrace{\mathbb{E}[R(s_t^M, a_t) - R'(s_t^M, a_t)]}_{\text{The impact of reward function differences}} + \underbrace{\mathbb{E}[R'(s_t^M, a_t) - R'(s_t^{M'}, a_t)]}_{\text{Reward differences caused by state differences}} \right) \\
 760 &\leq \sum_{t=0}^T \gamma^t (\Delta R + 2R_{\max} \cdot p_t) \\
 761 &= \frac{\Delta R}{1-\gamma} + \sum_{t=0}^T \gamma^t \cdot 2R_{\max} \cdot t \cdot \frac{\Delta P}{2} \\
 762 &= \frac{\Delta R}{1-\gamma} + R_{\max} \Delta P \sum_{t=0}^T t \gamma^t \\
 763 &= \frac{\Delta R}{1-\gamma} + R_{\max} \Delta P \cdot \frac{\gamma}{(1-\gamma)^2}
 \end{aligned} \tag{15}$$

775
 776 To estimate the variance of the cumulative reward difference, since the cumulative reward is bounded,
 777 its variance is also finite. We can easily obtain

$$778 |\Delta G| \leq G_{\max} = \frac{2R_{\max}}{1-\gamma} \tag{16}$$

781 According to Hoeffding:
 782

$$783 P(|\bar{\Delta G} - \mathbb{E}[\bar{\Delta G}]| \geq \epsilon) \leq 2 \exp\left(-\frac{2n\epsilon^2}{G_{\max}^2}\right) \tag{17}$$

786 Thus, with probability at least $1 - \delta$, we have:
 787

$$\begin{aligned}
 788 |\hat{Q}_M^n(s, a) - \hat{Q}_{M'}^n(s, a)| &\leq \mathbb{E}[|\Delta \bar{G}|] + G_{\max} \sqrt{\frac{\ln(2/\delta)}{2n}} \\
 789 &= \frac{\Delta R}{1-\gamma} + R_{\max} \Delta P \cdot \frac{\gamma}{(1-\gamma)^2} + \frac{2R_{\max}}{1-\gamma} \sqrt{\frac{\ln(2/\delta)}{2n}} \\
 790 &= \frac{1}{1-\gamma} (\Delta R + \frac{R_{\max}\gamma}{1-\gamma} \Delta P) + \frac{2R_{\max}}{1-\gamma} \sqrt{\frac{\ln(2/\delta)}{2n}} \\
 791 &= L(\Delta R + \kappa \Delta P) + L_2
 \end{aligned} \tag{18}$$

□

799 A.2 PROOF OF THEOREM 3.4

801 *Proof.* Proof of Theorem 3.4 First, we consider the case of a single MDP and assume that we have a
 802 “universal” upper bound $U(s, a) \geq Q_M^*(s, a)$.

803 **Lemma A.3.** Since $U(s, a) \geq Q_M^*$ holds for all (s, a) , and initially $Q(s, a) \leq U(s, a)$, for any
 804 update, $Q(s, a)$ maintains $Q(s, a) \leq U(s, a)$ and $Q(s, a) \geq$ (a non-negative expected estimate).

806 The above two points illustrate Since we update using $Q(s, a) = \min\{\hat{Q}(s, a), U(s, a)\}$ And since
 807 $U(s, a) \geq Q^*(s, a)$, during all sampling processes, if $\hat{Q}(s, a)$ overestimates $Q^*(s, a)$ significantly,
 808 it will still be truncated by $U(s, a)$, ensuring that $Q(s, a) \leq U(s, a)$. When $\hat{Q}(s, a)$ gradually
 809 approaches $Q^*(s, a)$, it will no longer be truncated. This does not hinder the convergence of Q to Q^* .

810
Theorem A.4 (Convergence in a Single MDP). *If there are infinitely many samples for each state s
811 and its available actions a (i.e., every branch in the MCTS search tree is "continuously" expanded),
812 then the $Q(s, a)$ generated by the above update formula almost surely converges to $Q_M^*(s, a)$.*
813

814 Now we aim to demonstrate that after completing certain MDPs (tasks) $\bar{M}_1, \bar{M}_2, \dots, \bar{M}_m$, and then
815 switching to a new MDP M , the algorithm achieves faster convergence.

816 First, we analyze the classic scenario without upper bounds. In a finite state-action space, to achieve
817 the desired outcome with high probability $1 - \delta$:

$$819 \quad \max_{(s, a) \in \mathcal{S} \times \mathcal{A}} |Q_n(s, a) - Q_M^*(s, a)| \leq \epsilon \quad (19)$$

821 The standard UCT/UCB theory typically provides a time complexity of $\tilde{O} \left(\frac{|\mathcal{S}||\mathcal{A}|}{(1-\gamma)^3 \epsilon^2} \ln \frac{1}{\delta} \right)$. To prove
822 this theorem, we just need to analyze the acceleration factor Γ , comparing the sampling complexity
823 of our aUCT and standard UCT.

825 More specifically, if we examine each specific (s, a) , the analysis often resembles that of multi-armed
826 bandits: for "suboptimal" (s, a) , approximately $\tilde{O} \left(\frac{1}{(\Delta_{(s, a)}^M)^2} \ln \frac{1}{\delta} \right)$ samples are required. Where
827 $\Delta_{(s, a)}^M = Q_M^*(s, a^*) - Q_M^*(s, a)$ is the value gap between the action and the optimal action. Summing
828 up the exploration costs for all state-action pairs gives a total magnitude of $\sum_{(s, a)} \frac{1}{(\Delta_{(s, a)}^M)^2}$.

831 Now we introduce the case with upper bounds and analyze how to reduce the number of samples
832 across different MDPs.

833 To quantitatively represent this acceleration, we divide the state-action pairs (s, a) into two groups:

835 \bullet \mathcal{S}_1 : Upper bounds are sufficiently tight and are truncated to be lower than the optimal action
836 from the very beginning.

$$838 \quad \mathcal{S}_1 = \{(s, a) | \exists i : U_{\bar{M}_i}(s, a) < Q_M^0(s, a)\} \quad (20)$$

840 \bullet \mathcal{S}_0 : The upper bounds are not "tight enough," i.e.,

$$841 \quad \mathcal{S}_0 = \text{remaining actions} \quad (21)$$

843 For $(s, a) \in \mathcal{S}_1$:

845 We treat each sampling as a multi-armed bandit. Let the true mean of the optimal arm be μ^* . For a
846 certain arm j , its true mean is known to satisfy $\mu_j \leq U_j < \mu^*$.

847 Even if we truncate $\hat{\mu}_n(j)$ at U_j , the UCB algorithm's "optimistic estimate" for this arm at step n is
848 still:

$$849 \quad Q_n(j) = \min \{\hat{\mu}_n(j), U_j\} + c \sqrt{\frac{\ln(n)}{N_j(n)}} \quad (22)$$

$$852 \quad U_j + c \sqrt{\frac{\ln(n)}{N_j(n)}} < \mu^* \quad (23)$$

855 Let $\Delta = \mu^* - U_j$. As long as:

$$857 \quad \sqrt{\frac{\ln(n)}{N_j(n)}} \leq \frac{\Delta}{2c} \quad (24)$$

859 From the above, it can be ensured that $Q_n(j)$ cannot exceed $\mu^* - \Delta/2$. So

$$861 \quad N_j(n) \geq \frac{4c^2 \ln(n)}{\Delta^2} \quad (25)$$

863 Where we obtain a sampling time complexity of $\tilde{O}(\ln n)$.

For $(s, a) \in \mathcal{S}_0$, these (s, a) cannot be pruned by "truncation." They still require multiple samples, as in classic UCT, to determine whether they are truly optimal. For any $(s, a) \in \mathcal{S}_0$, we still need approximately $\tilde{O}\left(\frac{1}{(\Delta_{(s,a)}^M)^2} \ln \frac{1}{\delta}\right)$ samples to distinguish that it is not as good as (s, a^*) . Thus, the sampling complexity of our algorithm is:

$$X_{\text{aUCT}} = \sum_{(s,a) \in \mathcal{S}_1} \tilde{O}(\ln n) + \sum_{(s,a) \in \mathcal{S}_0} \tilde{O}\left(\frac{1}{(\Delta_{(s,a)}^M)^2} \ln \frac{1}{\delta}\right), \quad (26)$$

Using the fact that $\tilde{O}(\ln n) \sim \tilde{O}(\ln \frac{1}{\delta})$, we can rewrite this as

$$X_{\text{aUCT}} = \sum_{(s,a) \in \mathcal{S}_1} \tilde{O}\left(\ln \frac{1}{\delta}\right) + \sum_{(s,a) \in \mathcal{S}_0} \tilde{O}\left(\frac{1}{(\Delta_{(s,a)}^M)^2} \ln \frac{1}{\delta}\right). \quad (27)$$

In contrast, the sampling complexity of the standard UCT can be obtained using the same analysis, i.e.,

$$X_{\text{UCT}} = \sum_{(s,a) \in \mathcal{S}_0 \cup \mathcal{S}_1} \tilde{O}\left(\frac{1}{(\Delta_{(s,a)}^M)^2} \ln \frac{1}{\delta}\right). \quad (28)$$

Comparing the order bounds from Equation (28) and Equation (27), we can find the acceleration factor Γ as

$$\Gamma = \frac{\sum_{(s,a) \in \mathcal{S}_1 \cup \mathcal{S}_0} \frac{1}{(\Delta_{(s,a)}^M)^2}}{\sum_{(s,a) \in \mathcal{S}_1} (1) + \sum_{(s,a) \in \mathcal{S}_0} \frac{1}{(\Delta_{(s,a)}^M)^2}}, \quad (29)$$

which is the desired result in the theorem. \square

A.3 PROOF OF THEOREM 4.1

Proof. Proof of Theorem 4.1 First, we need to establish unbiasedness and boundedness. For unbiasedness, we can derive:

$$\mathbb{E}[X_i] = \mathbb{E}_{(s,a) \sim \pi} \left[\frac{\mathcal{U}(s,a)}{\pi(s,a)} \cdot \Delta X(s,a) \right] = \mathbb{E}_{(s,a) \sim \mathcal{U}} [\Delta X(s,a)] = d(M, M') \quad (30)$$

Therefore, $\mathbb{E}[\hat{d}_{\mathcal{U}}] = d(M, M')$, meaning $\hat{d}_{\mathcal{U}}$ is an unbiased estimator.

$$w_i = \frac{\mathcal{U}(s_i, a_i)}{\pi(s_i, a_i)} \leq \frac{\mathcal{U}_{\max}}{\alpha} \quad (31)$$

Where $\mathcal{U}_{\max} = \max_{(s,a)} \mathcal{U}(s,a) = \frac{1}{|\mathcal{S}| \cdot |\mathcal{A}|}$. So we can get:

$$X_i = w_i \Delta X(s_i, a_i) \leq \left(\frac{\mathcal{U}_{\max}}{\alpha}\right) b \quad (32)$$

So we can get $X_i \in [0, C]$ where $C = \frac{\mathcal{U}_{\max}}{\alpha} b$.

Based on the above analysis, we have $\bar{X}_N = \frac{1}{N} \sum_{i=1}^N X_i = \hat{d}_{\mathcal{U}}$, $\mu = \mathbb{E}[X_i] = d(M, M')$. According to Hoeffding's inequality, for $\bar{X}_N \in [0, C]$, we have:

$$\Pr\{|\bar{X}_N - \mu| \geq \epsilon\} \leq 2 \exp\left(-\frac{2N\epsilon^2}{C^2}\right) \quad (33)$$

To achieve a confidence level of δ , it requires:

$$2 \exp\left(-\frac{2N\epsilon^2}{C^2}\right) \leq \delta \Leftrightarrow \exp\left(-\frac{2N\epsilon^2}{C^2}\right) \leq \frac{\delta}{2} \Leftrightarrow -\frac{2N\epsilon^2}{C^2} \leq \ln \frac{\delta}{2} \Leftrightarrow \frac{2N\epsilon^2}{C^2} \geq \ln \frac{2}{\delta} \Leftrightarrow N \geq \frac{C^2}{2\epsilon^2} \ln \frac{2}{\delta} \quad (34)$$

918 We get if fulfilled:

919
$$N \geq \frac{1}{2\epsilon^2} \left(\frac{\mathcal{U}_{\max}}{\alpha} b \right)^2 \ln \frac{2}{\delta} \quad (35)$$

920 There is then a high probability error upper bound:

921
$$\Pr\{|\hat{d}_{\mathcal{U}} - d(M, M')| \leq \epsilon\} \geq 1 - \delta \quad (36)$$

922 \square

923 **A.4 PROOF OF THEOREM 4.2**

924 *Proof.* Proof of Theorem 4.2 Constructing a martingale difference, let:

925
$$S_n := \sum_{k=1}^n (X_k - d(M, M')), Y_k := X_k - \mathbb{E}[X_k | \mathcal{F}_{k-1}] \quad (37)$$

926 According to the martingale condition in formula 9, we know that $Y_k = X_k - d(M, M')$, and
 927 $S_n = \sum_{k=1}^n Y_k$ satisfies $\mathbb{E}[Y_k | \mathcal{F}_{k-1}] = 0$. Thus, $\{S_n, \mathcal{F}_n\}$ is a martingale process.

928 Since $\pi_k(s, a) \geq \alpha \Rightarrow w_k \leq \frac{\mathcal{U}_{\max}}{\alpha}$, and $\Delta X(s, a) \leq b \Rightarrow X_k = w_k \Delta X(s_k, a_k) \leq \frac{\mathcal{U}_{\max}}{\alpha} b =: C$.
 929 Therefore, we have:

930
$$|Y_k| \leq \max\{X_k, d(M, M')\} \leq C \quad (38)$$

931 According to the Azuma-Hoeffding inequality for bounded martingale differences, we have:

932
$$\Pr\{|S_n| \geq t\} \leq 2 \exp\left(-\frac{t^2}{2NC^2}\right) \quad (39)$$

933 Let $t = N\epsilon$, then $|S_n| \geq t$ is equivalent to $|\sum_{k=1}^n X_k - Nd(M, M')| \geq N\epsilon$, that is:

934
$$|\hat{d}_{\mathcal{U}}^{(n)} - d(M, M')| \geq \epsilon \quad (40)$$

935 So:

936
$$\Pr\{|\hat{d}_{\mathcal{U}}^{(N)} - d(M, M')| \geq \epsilon\} \leq 2 \exp\left(-\frac{N\epsilon^2}{2C^2}\right) \quad (41)$$

937 Thus, as long as $N \geq \frac{2C^2}{\epsilon^2} \ln \frac{2}{\delta}$, we have $\Pr\{|\hat{d}_{\mathcal{U}}^{(N)} - d(M, M')| \geq \epsilon\} \leq \delta$. \square

938 **A.5 PROOF OF THEOREM 4.3**

939 *Proof.* Proof of Theorem 4.3 We decompose $d_{\mathcal{U}}$.

940
$$\begin{aligned} d_{\mathcal{U}}(M, M_i) &= \mathbb{E}_{(s, a) \sim \mathcal{U}} [\underbrace{|R_s^a - R_s^{a, (i)}|}_{\text{Reward difference}} + \underbrace{\kappa \sum_{s'} |P_{ss'}^a - P_{ss'}^{a, (i)}|}_{\text{transition difference}}] \\ &\simeq \mathbb{E}_{(s, a) \sim \mathcal{U}} [|R_s^a - R_s^{a, (i)}| + \kappa \|\Psi_{\phi}(s, a) - \Psi_{\phi_i}(s, a)\|_1] \\ &\leq \mathbb{E}_{(s, a) \sim \mathcal{U}} [L_3 \rho(\phi, \phi_i) + \kappa L_3 \rho(\phi, \phi_i)] \\ &\leq L_3 \rho(\phi, \phi_i) + \kappa L_3 \rho(\phi, \phi_i) \\ &= (1 + \kappa) L_3 \rho(\phi, \phi_i) \\ &= (1 + \kappa) L_3 \hat{d}_{\text{para}}(M, M_i) \end{aligned} \quad (42)$$

941 \square

942 **B PSEUDO-CODE**

943
 944
 945
 946
 947
 948
 949
 950
 951
 952
 953
 954
 955
 956
 957
 958
 959
 960
 961
 962
 963
 964
 965
 966
 967
 968
 969
 970
 971

972

973

974

975

976

977

978

979

980

981

982

Algorithm 1 UMCTS

983 **Require:** $\{\mathcal{M}_1, \dots, \mathcal{M}_M\}, \mathcal{U}, \kappa, L, L_2^{(i)}, \gamma, R_{\max}, C, T$

984 1: **for** $i = 1$ to M **do**

985 2: Repeat sampling (s, a) from the uniform distribution \mathcal{U} to update R and P .

986 3: **for** $j = 1$ to M **do**

987 4: $d(\mathcal{M}_i, \mathcal{M}_j) \leftarrow \mathbb{E}_{(s, a, s') \sim \mathcal{U}} [|R_s^a - \bar{R}_s^a| + \kappa |P_{ss'}^a - \bar{P}_{ss'}^a|]$

988 5: **end for**

989 6: Initialize root node s_0 , set $N(\cdot), N(\cdot, \cdot), W(\cdot, \cdot)$ to 0

990 7: **for** $t = 1$ to T **do**

991 8: **Selection:**

992 9: Set current node $s \leftarrow s_0$

993 10: **while** child nodes of s are fully expanded **do**

994 11: Choose $a = \operatorname{argmax}_a (Q(s, a))$ // using Eq. (*) below

995 12: $s \leftarrow$ child node after action a

996 13: **end while**

997 14: **Expansion:**

998 15: Expand one non-visited action a_{new} at s , sample s' from environment or model

999 16: Create new child node s' , set $N(s', \cdot) = 0, W(s', \cdot) = 0$

1000 17: **Simulation:**

1001 18: Perform a (light) rollout or default policy from s' to terminal or horizon

1002 19: Receive cumulative reward G

1003 20: **Backpropagation:**

1004 21: Traverse back from s' to s_0 along visited path

1005 22: **for all** visited state-action pairs (\tilde{s}, \tilde{a}) **do**

1006 23: $N(\tilde{s}) \leftarrow N(\tilde{s}) + 1$

1007 24: $N(\tilde{s}, \tilde{a}) \leftarrow N(\tilde{s}, \tilde{a}) + 1$

1008 25: $W(\tilde{s}, \tilde{a}) \leftarrow W(\tilde{s}, \tilde{a}) + G$

1009 26: // Update $Q(\tilde{s}, \tilde{a})$ with UMCTS bound:

1010 27: $U_{\bar{\mathcal{M}}}(\tilde{s}, \tilde{a}) \leftarrow Q_{\bar{\mathcal{M}}}^*(\tilde{s}, \tilde{a}) + L \cdot d(\mathcal{M}, \bar{\mathcal{M}}) + L_2^{(i)}$

1011 28: $U(\tilde{s}, \tilde{a}) \leftarrow \min\left\{\frac{R_{\max}}{1-\gamma}, U_{\bar{\mathcal{M}}}(\tilde{s}, \tilde{a}), \dots\right\}$

1012 29: $Q(\tilde{s}, \tilde{a}) \leftarrow \min\left\{\frac{W(\tilde{s}, \tilde{a})}{N(\tilde{s}, \tilde{a})} + C \sqrt{\frac{\ln N(\tilde{s})}{N(\tilde{s}, \tilde{a})}}, U(\tilde{s}, \tilde{a})\right\} \quad (*)$

1013 30: **end for**

1014 31: **end for**

1015 32: **end for**

1016

1017

1018

1019

1020

1021

1022

1023

1024

1025

1026
1027 **Algorithm 2** UMCTS with Importance Sampling
1028 **Require:** Tasks $\{\mathcal{M}_1, \dots, \mathcal{M}_M\}$, each partially known; Uniform distribution $\mathcal{U}(s, a)$; Lipschitz
1029 constants $L, L_2^{(i)}$; Discount factor γ , maximum reward R_{\max} ; Exploration constant C ; Number
1030 of search iterations T ; A (default) policy π used in Simulation for importance sampling;
1031 1: **Function** DISTANCE($\mathcal{M}, \bar{\mathcal{M}}, \pi$):
1032 2: $\Delta X(s, a) \triangleq \Delta R_s^a + \kappa \Delta P_s^a$
1033 3: **return** $\mathbb{E}_{(s,a) \sim \pi} \left[\frac{\mathcal{U}(s, a)}{\pi(s, a)} \cdot \Delta X(s, a) \right]$
1034 4: // For each task \mathcal{M}_i
1035 5: **for** $i = 1$ to M **do**
1036 6: Initialize root node s_0 , set $N(\cdot) = 0, N(\cdot, \cdot) = 0, W(\cdot, \cdot) = 0$
1037 7: (Optionally maintain a buffer \mathcal{D}_i for storing samples (s,a))
1038 8: **for** $t = 1$ to T **do**
1039 9: **Selection:**
1040 10: $s \leftarrow s_0$
1041 11: **while** all actions from s are fully expanded **and** s not terminal **do**
1042 12: $a \leftarrow \text{argmax } (Q(s, a))$ // UCB or UMCTS criterion
1043 13: $s \leftarrow$ child node after action a
1044 14: **end while**
1045 15: **Expansion:**
1046 16: **if** s not terminal **then**
1047 17: Choose one unvisited action a_{new} at s
1048 18: Sample next state $s' \sim P_i(\cdot | s, a_{\text{new}})$ // from environment or model
1049 19: Create child node s' , set $N(s', \cdot) = 0, W(s', \cdot) = 0$
1050 20: **end if**
1051 21: **Simulation:**
1052 22: Initialize cumulative reward $G \leftarrow 0$
1053 23: $s_{\text{sim}} \leftarrow s'$
1054 24: **while** s_{sim} is not terminal **do**
1055 25: Pick action a_{sim} by policy $\pi(\cdot | s_{\text{sim}})$
1056 26: Observe reward $r_{\text{sim}} = R_i(s_{\text{sim}}, a_{\text{sim}})$
1057 27: Observe next state $s_{\text{next}} \sim P_i(\cdot | s_{\text{sim}}, a_{\text{sim}})$
1058 28: $G \leftarrow G + r_{\text{sim}}$
1059 29: // Update or record increments for $R_s^a, P_{s,s'}^a$
1060 30: $\Delta R_{s_{\text{sim}}}^a, \Delta P_{s_{\text{sim}}}^a \leftarrow$ (computed from new sample)
1061 31: // Optionally store $(s_{\text{sim}}, a_{\text{sim}})$ in \mathcal{D}_i for importance sampling
1062 32: $s_{\text{sim}} \leftarrow s_{\text{next}}$
1063 33: **end while**
1064 34: **Backpropagation:**
1065 35: Traverse from s' back to s_0 along visited path
1066 36: **for** all visited pairs (\tilde{s}, \tilde{a}) **do**
1067 37: $N(\tilde{s}) \leftarrow N(\tilde{s}) + 1$
1068 38: $N(\tilde{s}, \tilde{a}) \leftarrow N(\tilde{s}, \tilde{a}) + 1$
1069 39: $W(\tilde{s}, \tilde{a}) \leftarrow W(\tilde{s}, \tilde{a}) + G$
1070 40: /* Use the Lipschitz bound with distance estimation */
1071 41: $d(\mathcal{M}_i, \bar{\mathcal{M}}) \leftarrow \text{Distance}(\mathcal{M}_i, \bar{\mathcal{M}}, \pi)$
1072 42: $U_{\bar{\mathcal{M}}}(\tilde{s}, \tilde{a}) \leftarrow Q_{\bar{\mathcal{M}}}^*(\tilde{s}, \tilde{a}) + L \cdot d(\mathcal{M}_i, \bar{\mathcal{M}}) + L_2^{(i)}$
1073 43: $U(\tilde{s}, \tilde{a}) \leftarrow \min \left\{ \frac{R_{\max}}{1 - \gamma}, U_{\bar{\mathcal{M}}}(\tilde{s}, \tilde{a}), \dots \right\}$
1074 44: /* UMCTS update rule */
1075 45: $Q(\tilde{s}, \tilde{a}) \leftarrow \min \left\{ \frac{W(\tilde{s}, \tilde{a})}{N(\tilde{s}, \tilde{a})} + C \sqrt{\frac{\ln N(\tilde{s})}{N(\tilde{s}, \tilde{a})}}, U(\tilde{s}, \tilde{a}) \right\} \quad (*)$
1076 46: **end for**
1077 47: **end for**
1078 48: **end for**

1080

1081

Algorithm 3 UMCTS with Neural Network Environment Model

Require: MDPs $\{\mathcal{M}_1, \dots, \mathcal{M}_M\}$, each with trained neural network parameters $\{\phi_1, \dots, \phi_M\}$;
 A new MDP M (partially known), with neural network $\Psi_\phi : \mathcal{S} \times \mathcal{A} \rightarrow \Delta(\mathcal{S})$; A distance
 function $\rho(\phi, \phi_i) \geq 0$ on parameter space (e.g., ℓ_2 -norm); Define $\hat{d}_{para}(M, M_i) = \rho(\phi, \phi_i)$;
 Lipschitz constants $L, L_2^{(i)}$, discount factor γ , R_{\max} , exploration constant C , iterations T ; A
 default (simulation) policy π for rollouts

1: // For each task M (with parameter ϕ) run UMCTS
 2: Initialize root node s_0 , counters $N(\cdot) = 0$, $N(\cdot, \cdot) = 0$, $W(\cdot, \cdot) = 0$
 3: **for** $t = 1$ to T **do**
 4: **Selection:**
 5: $s \leftarrow s_0$
 6: **while** all actions from s are expanded **and** s not terminal **do**
 7: $a \leftarrow \text{argmax } (Q(s, a))$
 8: $s \leftarrow$ child node after action a
 9: **end while**
 10: **Expansion:**
 11: **if** s not terminal **then**
 12: choose an unvisited action a_{new}
 13: sample $s' \sim \Psi_\phi(\cdot | s, a_{\text{new}})$ // neural net predicts next state distribution
 14: create child node s'
 15: $N(s', \cdot) \leftarrow 0$, $W(s', \cdot) \leftarrow 0$
 16: **end if**
 17: **Simulation:**
 18: $G \leftarrow 0$
 19: $s_{\text{sim}} \leftarrow s'$
 20: **while** s_{sim} not terminal **do**
 21: $a_{\text{sim}} \leftarrow$ sample from $\pi(\cdot | s_{\text{sim}})$
 22: // observe reward (possibly from real env or approximated by a learned reward model)
 23: $r_{\text{sim}} = R(s_{\text{sim}}, a_{\text{sim}})$
 24: $s_{\text{next}} \sim \Psi_\phi(\cdot | s_{\text{sim}}, a_{\text{sim}})$
 25: $G \leftarrow G + r_{\text{sim}}$
 26: /* update ϕ via gradient (e.g. supervised/unsupervised RL objective) */
 27: $\phi \leftarrow \phi - \eta \nabla_\phi \mathcal{L}(\phi; (s_{\text{sim}}, a_{\text{sim}}, s_{\text{next}}))$
 28: $s_{\text{sim}} \leftarrow s_{\text{next}}$
 29: **end while**
 30: **Backpropagation:**
 31: traverse from s' back to s_0
 32: **for all** visited state-action pairs (\tilde{s}, \tilde{a}) **do**
 33: $N(\tilde{s}) \leftarrow N(\tilde{s}) + 1$
 34: $N(\tilde{s}, \tilde{a}) \leftarrow N(\tilde{s}, \tilde{a}) + 1$
 35: $W(\tilde{s}, \tilde{a}) \leftarrow W(\tilde{s}, \tilde{a}) + G$
 36: // parametric distance to previously trained model ϕ_i
 37: $\hat{d}_{para}(M, M_i) \triangleq \rho(\phi, \phi_i)$
 38: // Lipschitz-based upper bound
 39: $U_{\bar{\mathcal{M}}}(\tilde{s}, \tilde{a}) \leftarrow Q_{\bar{\mathcal{M}}}^*(\tilde{s}, \tilde{a}) + L \cdot \hat{d}_{para}(M, \bar{\mathcal{M}}) + L_2^{(i)}$
 40: $U(\tilde{s}, \tilde{a}) \leftarrow \min \left\{ \frac{R_{\max}}{1-\gamma}, U_{\bar{\mathcal{M}}}(\tilde{s}, \tilde{a}), \dots \right\}$
 41: // UMCTS update rule
 42: $Q(\tilde{s}, \tilde{a}) \leftarrow \min \left\{ \frac{W(\tilde{s}, \tilde{a})}{N(\tilde{s}, \tilde{a})} + C \sqrt{\frac{\ln N(\tilde{s})}{N(\tilde{s}, \tilde{a})}}, U(\tilde{s}, \tilde{a}) \right\} \quad (*)$
 43: **end for**
 44: **end for**

1133